GEOPHYSICAL RESEARCH LETTERS, VOL. 35, L20311, doi:10.1029/2008GL035326, 2008

Regional conductivity structure of Cascadia: Preliminary results from 3D inversion of USArray transportable array magnetotelluric data

Prasanta K. Patro[1,2] and Gary D. Egbert[1]

Received 11 July 2008; revised 27 September 2008; accepted 1 October 2008; published 31 October 2008.

[1] In conjunction with the USArray component of EarthScope, long period magnetotelluric (MT) data are being acquired in a series of arrays across the continental US. Initial deployments in 2006 and 2007 acquired data (10–10,000 s) at 110 sites covering the US Pacific Northwest, distributed with the same nominal spacing as the USArray seismic transportable array (∼75 km). The most striking and robust features revealed by initial three-dimensional inversion of this dataset are extensive areas of high conductivity in the lower crust beneath all of southeastern Oregon, and beneath the Cascade Mountains, contrasting with very resistive crust in Siletzia and the Columbia Embayment. Significant variations in upper mantle conductivity are also revealed by the inversions, with the most conductive mantle beneath the Washington backarc, and the most resistive corresponding to subducting oceanic mantle. **Citation:** Patro, P. K., and G. D. Egbert (2008), Regional conductivity structure of Cascadia: Preliminary results from 3D inversion of USArray transportable array magnetotelluric data, *Geophys. Res. Lett.*, *35*, L20311, doi:10.1029/2008GL035326.

1. Introduction

[2] The USArray component of EarthScope is a continental-scale geophysical observational program that will provide new constraints on the structure and evolution of the North American continent. As an adjunct to the seismic transportable array (TA), which over the next decade will cover the continental US with temporary seismic observatories at an approximate spacing of 75 km, long period (10–20,000 s) magnetotelluric (MT) data will be acquired in selected areas, with comparable site densities. The first MT TA data were acquired at 30 sites in eastern Oregon in the summer of 2006, followed by 80 sites covering western Oregon, all of Washington State and western Idaho in summer 2007. In contrast to traditional MT surveys, where sites are concentrated along one or a few profiles, sites were widely spaced to provide quasi-uniform coverage of the entire area. This array configuration, and the geologic complexity of the study area (Figure 1), effectively demands a three-dimensional (3D) interpretation. Here we present the results of our preliminary efforts in this direction.

[3] The MT array traverses a wide range of geologic environments, from the subducting Juan de Fuca (JDF) plate in the west, across the Cascade volcanic arc, and into the Columbia Plateau, High Desert, western Snake River Plain and Northwest Basin and Range provinces to the east. The modern position of the subduction zone dates from approximately 48 Ma, when a large fragment of thickened oceanic lithosphere was accreted to the Pacific Northwest margin [*Madsen et al.*, 2006] near the end of Laramide orogeny. This accreted oceanic terrane, which fills the Columbia Embayment and forms the modern forearc basement in NW Oregon and SW Washington, is sometimes referred to loosely as Siletzia (e.g., E. Humphreys, Relation of flat subduction to magmatism and deformation in the western USA, submitted to *Backbone of the Americas*, 2008). From 17 to 12 million years ago, great flood basalts (over 200,000 km^3) erupted in Washington and Oregon, covering much of the Columbia Plateau [*Camp and Ross*, 2004]. These eruptions have been followed by age progressive silicic volcanism which continues to the present day and has resulted in the Snake River Plain (terminating in the east at Yellowstone [*Pierce and Morgan*, 1992]) and the High Lava Plains of eastern Oregon (terminating in the west at Newberry Volcano [*Jordan et al.*, 2004]).

[4] In a broader context, much of the crust in the Western US is rapidly deforming, with widespread extension in the Basin and Range (BR), which the southeast corner of the array intersects, and a broad zone of right-lateral shear to the south extending from the San Andreas Fault deep into the continental interior [*Humphreys and Coblentz*, 2007]. In contrast, Siletzia has retained sufficient strength to avoid deformation, accommodating right-lateral shear through clockwise block rotation which continues to this day [*Wells et al.*, 1998, *McCaffrey et al.*, 2007].

2. Magnetotelluric Data and Analysis

[5] MT data were acquired by a commercial contractor (GSY-USA) using conventional long period MT instruments based on fluxgate magnetometers. Time series data (typically of three weeks duration) were processed using a standard robust remote reference approach [*Egbert*, 1997], resulting in most cases in smooth response curves over the period range 10–10,000 s. Although there are significant site-to-site static shifts in apparent resistivities [e.g., *Bahr and Simpson*, 2005], spatial maps of phases are generally well behaved, and exhibit large scale coherent features (see auxiliary material[1], Figures S1 and S2).

[6] Induction vectors, which are computed from the ratio of vertical to horizontal magnetic field components, are indicative of lateral conductivity contrasts. For the Cascadia array these are strongly affected by the ocean in the western part of the array, but also reveal other substantial conductive

[1]College of Oceanic and Atmospheric Sciences, Oregon State University, Corvallis, Oregon, USA.
[2]Now at National Geophysical Research Institute, Hyderabad, India.

0094-8276/08/2008GL035326$05.00

[1]Auxiliary materials are available in the HTML. doi:10.1029/2008GL035326.

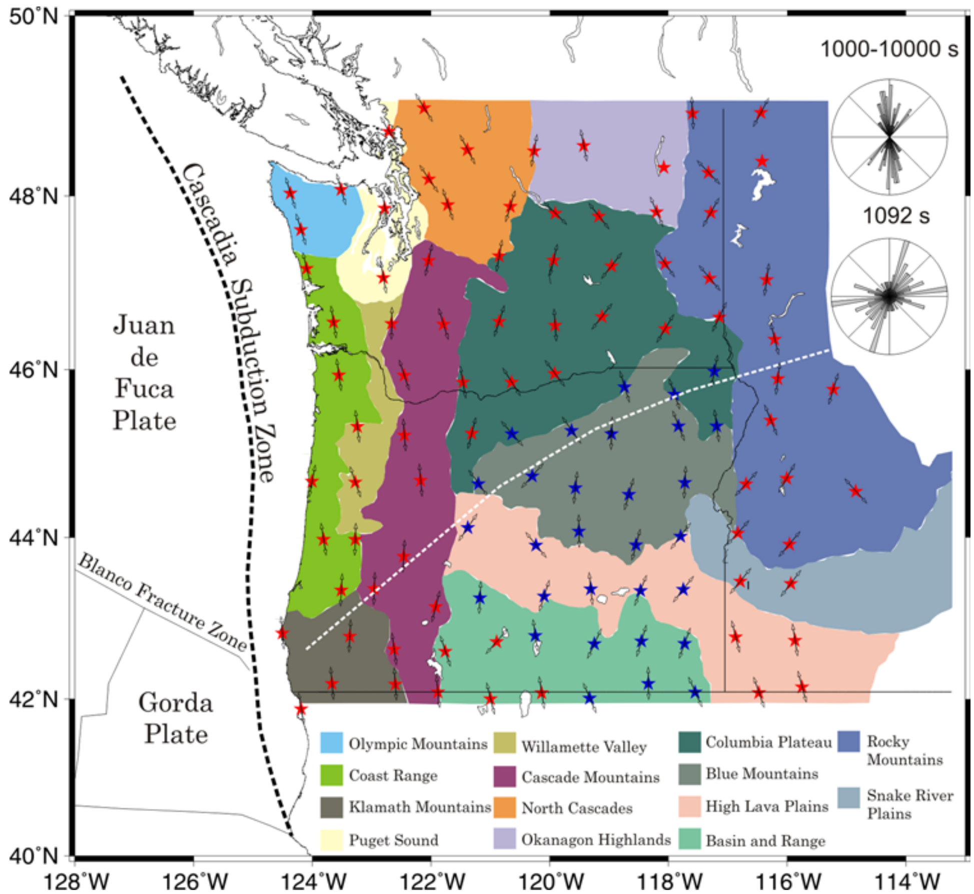

Figure 1. Location of MT sites collected in 2006 (blue stars) and 2007 (red stars) on a map of physiographic provinces [after *Rosenfeld*, 1985]. Black arrows give geo-electric strike directions determined by fitting the distortion model of *Smith* [1997] for periods of 1000–10000 s. The top inset shows the distribution of strike directions, which have a 90° ambiguity. The bottom inset is a rose diagram for real induction vectors, which point towards conductive features, for a period of 1092 s.

anomalies with varying orientations, as summarized in Figure 1 (bottom inset). Geo-electric strike analysis based on tensor decomposition [e.g., *Smith*, 1997] further confirms (Figure 1, top inset) that there is no consistent geo-electric strike that would allow two-dimensional interpretation of this dataset.

3. 3D inversion

[7] We used WSINV3D, a 3-D regularized inversion program [*Siripunvaraporn et al.*, 2005], to fit the 4 complex impedance tensor components for the 109 sites with data of acceptable quality. The model domain has total dimensions 1460 × 1590 × 550 km consisting of N_x = 80, N_y = 78 horizontal grid cells with nominal grid spacing in the central part of the domain approximately 12 km. The Pacific Ocean, with realistic bathymetry and conductivity (3.33 S/m), extends 480 km west of the coast. In the vertical the mesh has N_z = 34 layers, plus 7 additional layers for the air. Impedances for 8 periods (100–8000 s) were selected for inversion. Even for this relatively limited data subset and coarse model resolution the serial inversion code required 11 days per (outer loop) iteration on a single (2.8 GHz) processor PC, using essentially all of the 16 Gb of available RAM.

[8] Actual impedance estimation errors were used to normalize data misfits, and a half space of 100 ohm-m (except for the ocean) was used as a prior. As discussed in the auxiliary material, we experimented with several variants on the model covariance. The smoothest inverse solution, computed with larger horizontal decorrelation length scales, is shown in Figure 2. Alternate runs with less horizontal smoothing fit the data somewhat better (Figure S3), but all inverse solutions were qualitatively similar, particularly with regard to the large scale features emphasized below. The computed responses fit the observed signal well for periods up to a few thousand seconds (Figure S1). At longer periods fits are poorer, particularly for some sites near the coast (Figure S2). We also verified, by forward modeling, that the induction vectors were fit at least qualitatively by the inverse solutions.

4. Results and Interpretation

[9] The most prominent feature revealed by the inversion is an extensive lower crustal conductor (C1 in Figure 2), which occupies the triangular region southeast of the dotted white line extending from the coast near the California border to the eastern edge of the array, near the Oregon-Washington border (Figures 1 and 2). This conductive

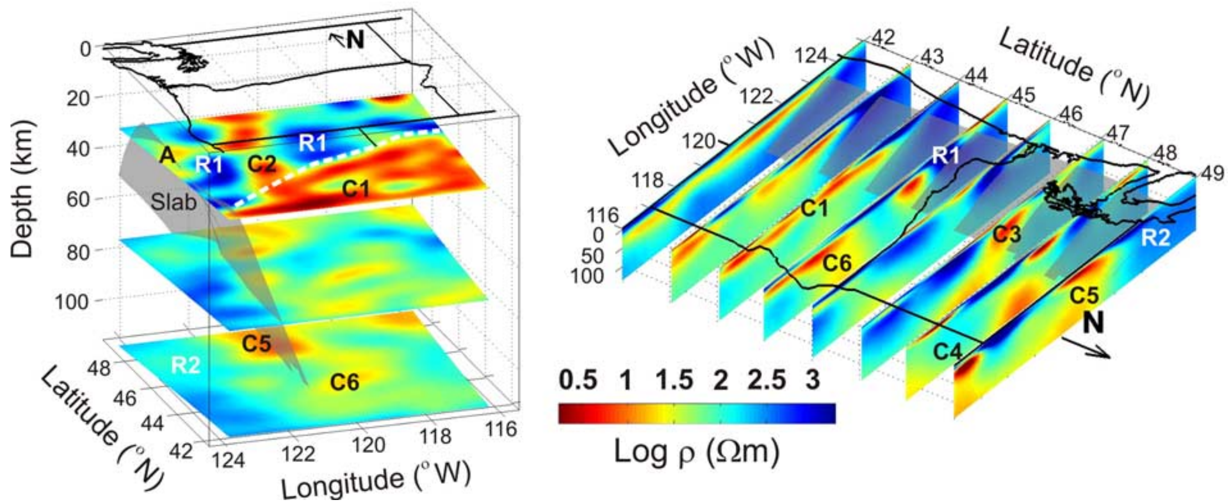

Figure 2. 3D resistivity image of the Pacific Northwest USA derived from the 3D inversion, plotted as slices of (left) constant depth and (right) constant latitude. Slab geometry from *McCrory et al.* [2003]. A: conductive zone in the forearc; C1–C6 and R1–R2 conductive and resistive features discussed in the text.

feature extends beneath the northwest BR, High Lava Plains, Western Snake River Plain, and Blue Mountains. The contact between C1 and more resistive crust to the northwest is interpreted as the southern boundary of the oceanic accreted terrane, i.e., Siletzia. Vertical conductivity profiles for selected physiographic provinces (Figure 1), computed by geographic averaging of the 3D inversion results, are given in Figure 3. The integrated conductance of the lower crustal layers is over 3000 S beneath the NWBR, and somewhat less to the north. In the NWBR in particular the zone of high conductivity appears to extend into the upper mantle, but further analysis will be required to verify this possibility.

[10] Based on higher frequency MT studies across the Cascade Range and surrounding geological provinces, *Stanley et al.* [1990] inferred a zone of high conductivity in southeastern Oregon below depths of about 15–20 km. Our results refine this picture significantly, revealing the broad spatial extent, approximate thickness, and high total conductance of this layer, which is quite similar in these respects to those seen in the lower crust elsewhere in the BR, and most probably reflects similar processes. *Wannamaker et al.* [2008] infer a lower crustal conductance in the eastern Great Basin and Transition Zone of ~3000 S and suggest that these high conductivities result from magmatic underplating associated with BR extension. As upward migrating magmas crystallize at the base of the crust several volume percent of H_2O-CO_2, highly saline brines are exsolved. With appropriate (interconnected) pore geometry these fluids (possibly with some contribution from partial melt near the moho) can easily account for the observed high conductivities [*Wannamaker et al.*, 2008].

[11] Note that the lower crustal conductor extends northward beyond what is normally considered to be the BR, albeit with reduced amplitude. This is consistent with the interpretation of Humphreys (submitted manuscript, 2008) that the interior shear zone in California broadens across NW Nevada and SE Oregon to accommodate rotation of the large strong crustal block that is Siletzia, resulting in faults of releasing orientation, and effective integration of this zone with Basin and Range extension (Humphreys, submitted manuscript, 2008). The zone of enhanced lower crustal conductivity thus correlates with weakened continental crust, and coincides with the zone of active crustal deformation.

[12] An elongate (N–S) conductive zone in the lower crust beneath the Cascade axis is also delineated (C2–C3 in Figure 2). This feature, which exhibits significant variability

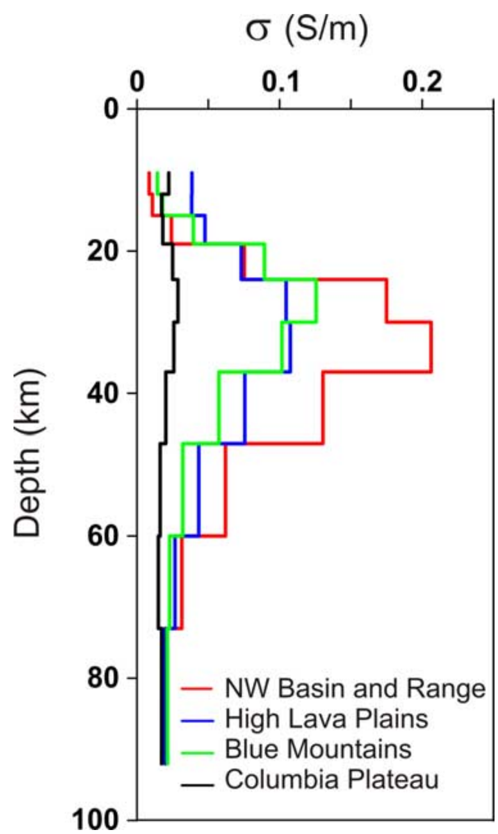

Figure 3. Vertical conductivity profiles for selected physiographic provinces.

along axis, also most likely reflects the presence of interconnected fluids, in this case from the subducting slab [*Wannamaker et al.*, 1989]. In central Oregon, near where the EMSLAB MT profile also imaged a zone of high conductivity in the lower crust beneath the high Cascades [*Wannamaker et al.*, 1989], C2 extends deeper, and merges with the lower crustal conductor to the east. In the north the Cascades conductive anomaly is more pronounced, and extends into the upper crust (C3 in Figure 2, right) where it coincides with the Southwest Washington Cascades Conductor (SWCC) [*Stanley et al.*, 1990; *Egbert and Booker*, 1993]. Similar to *Stanley et al.* [1990], the SWCC appears in the 3D model as an upper crustal feature just west of the Cascades, but then dips to the east, possibly even connecting to high conductivities in the upper mantle beneath the Columbia Plateau. The shallow part of the SWCC was interpreted by *Stanley et al.* [1990] to be a late Createaceous to early Eocene forearc basin and accretionary prism system sutured against pre-Eocene North America during accretion of Siletzia. It is likely that the deeper parts of the SWCC have a distinct cause (i.e., fluids associated with subduction and arc magmatism), given the near ubiquity of high conductivities beneath the arc.

[13] Most of the forearc is highly resistivity (R1) coinciding with the thick crust and high seismic velocities [*Parsons et al.*, 1999] of the Siletz terrane. There is some suggestion of higher conductivity above the slab further to the west, along much of the margin (A in Figure 2). This would be consistent with the zone of low resistivity imaged above the JDF plate by the EMSLAB MT profile which *Wannamaker et al.* [1989] inferred to be due to dewatering of subducted sediments (and possibly also mineral dehydration), but it may also result from accreted marine sedimentary rocks in the deformation front offshore. Given the wide station spacing and limited high frequency content of the data used for the 3D inversion, such (important) details are poorly resolved.

[14] There are several other zones of enhanced crustal conductivity evident in Figure 2. For example, a crustal conductor (C4) is evident near the northeast corner of the array. This feature appears to be shallower (upper crustal) near the Canadian border, but deepens as it extends to the southeast to at least 47.5N, where it perhaps then connects to more conductive features in the mantle. A similar crustal feature was identified by *Gough et al.* [1989] from EMSLAB magnetic variation array data as the southern termination of a prominent conductive feature (the Southern Alberta-British Columbia conductor) mapped in Canada with MV array data. High conductivity in the upper crust is also evident in the core rocks of the Olympic peninsula (47–48N, near the Pacific coast [*Aprea et al.*, 1998]).

[15] The oceanic mantle subducting beneath the North American continent is clearly more resistive (R2) than the adjacent continental mantle, to depths of at least 150 km. Perhaps the most striking feature in the mantle is a zone of high conductivity (C5) in the Washington backarc above the subducting JDF plate. This is consistent with elevated mantle conductivities reported for MT profiles just to the north by *Soyer and Unsworth* [2006], who suggested shallow convecting asthenosphere [*Currie et al.*, 2004] as the cause. To the extent that C5 continues at all into Oregon, this feature has reduced amplitude, and appears broken up and shifted to the east. There is also a circular conducting feature surrounded by a ring of more resistive mantle in central Oregon (C6). This pattern is qualitatively similar to variations in seismic velocities imaged by *Roth et al.* [2008] at similar mantle depths beneath Oregon. However, C6 is offset somewhat to the northeast relative to the lowest seismic velocities, which appear directly beneath Newberry Caldera, and were inferred to result from partial melts, concentrated in this area due to the combination of fluids released from the downgoing slab and elevated asthenospheric mantle temperatures beneath the High Lava Plains. These deeper mantle features in the resistivity images deserve more careful investigation, including further tests to verify that they are truly required of the data, and how well their position is resolved.

5. Conclusions

[16] In spite of the wide site spacing and limited control over near-surface distorting structures, a very sensible and coherent large scale picture of regional scale conductivity variations in the Pacific NW US results from 3D inversion of the USArray TA MT data. Major crustal features in the 3D inverse solution are generally consistent with previous higher resolution EM investigations in Cascadia [e.g., *Wannamaker et al.*, 1989; *Stanley et al.*, 1990], but the broad spatial coverage provides valuable new insights into the geoelectric structure of the region. *Gough et al.* [1989] inferred many of the same large scale features from the EMSLAB MV array, including the relatively conductive NWBR and Cascades. However, the interpretation by these authors was necessarily more qualitative, with very limited depth resolution—e.g., they inferred that the NWBR conductor was in the mantle, and they had no constraint on its conductance. The view of the mantle provided here, with a very clear delineation of more resistive oceanic mantle, and the variation of backarc conductivity from north to south, are in fact more novel, as previous MT investigations in this area have not had sufficient aperture to effectively explore to these depths. However, these deeper features have a more subtle expression in the MT data, and data fits are poorer at long periods. Further inversion studies, including exploration of issues of mantle anisotropy, are clearly warranted.

[17] While resolution of fine scale details, especially in the upper crust, will clearly be limited by the wide station spacing and the lack of high frequency data that will be collected by USArray, our initial inversion results are extremely encouraging. The regional scale MT array data that will be collected over the next few years, will, in conjunction with further development of 3D inversion capabilities, provide important new constraints on physical state and composition—in particular with regard to fluid content—of the North American crust and upper mantle.

[18] **Acknowledgments.** Thanks to Weerachai Siripunvaraporn for providing the 3D inversion code. Support for P. K. Patro while at Oregon State University was made possible through grants to G. D. Egbert from the National Science Foundation (NSF-EAR0345438) and the U.S. Department of Energy (DE-FG02-06ER15819).

References

Aprea, C., M. Unsworth, and J. Booker (1998), Resistivity structure of the Olympic Mountains and Puget Lowlands, *Geophys. Res. Lett.*, *25*, 109–112.

Bahr, K., and F. Simpson (2005), *Practical Magnetotellurics*, 270 pp., Cambridge Univ. Press, Cambridge, U. K.
Camp, V. E., and M. E. Ross (2004), Mantle dynamics and genesis of mafic magmatism in the intermontane Pacific Northwest, *J. Geophys. Res.*, *109*, B08204, doi:10.1029/2003JB002838.
Currie, C. A., K. Wang, R. D. Hyndman, and J. He (2004), The thermal effects of steady-state slab-driven mantle flow above a subducting plate: The Cascadia subduction zone and backarc, *Earth. Planet. Sci. Lett.*, *223*, 35–48.
Egbert, G. D. (1997), Robust multiple-station magntotelluric data processing, *Geophys J. Int.*, *130*, 475–496.
Egbert, G. D., and J. R. Booker (1993), Imaging crustal structure in southwestern Washington with small magnetometer arrays, *J. Geophys. Res.*, *98*(B9), 15,967–15,985.
Gough, D. I., D. M. McKirdy, D. V. Woods, and H. Geiger (1989), Conductive structures and tectonics beneath the EMSLAB land array, *J. Geophys. Res.*, *94*(B10), 14,099–14,110.
Humphreys, E. D., and D. D. Coblentz (2007), North American dynamics and western U.S. tectonics, *Rev. Geophys.*, *45*, RG3001, doi:10.1029/2005RG000181.
Jordan, B. T., A. L. Grunder, R. A. Duncan, and A. L. Deino (2004), Geochronology of age-progressive volcanism of the Oregon High Lava Plains: Implications for the plume interpretation of Yellowstone, *J. Geophys. Res.*, *109*, B10202, doi:10.1029/2003JB002776.
Madsen, J. K., D. J. Thorkelson, R. M. Friedman, and D. D. Marshall (2006), Cenozoic to Recent configuration in the Pacific Basin: Ridge subduction and slab window magmatism in western North America, *Geosphere*, *2*, 11–34, doi:10.1130/GES00020.1.
McCaffrey, R., A. I. Qamar, R. W. King, R. Wells, G. Khazaradze, C. A. Williams, C. W. Stevens, J. J. Vollick, and P. C. Zwick (2007), Fault locking, block rotation and crustal deformation in the Pacific Northwest, *Geophys. J. Int.*, *169*, 1315–1340.
McCrory, P. A., J. L. Blair, D. H. Oppenheimer, and S. R. Walter (2003), Depth to the Juan de Fuca slab beneath the Cascadia subduction margin: A 3-D model for sorting earthquakes [CD-ROM], *U.S. Geol. Surv. Digital Data Ser.*, *1*.
Parsons, T., R. E. Wells, M. A. Fisher, E. Flueh, and U. S. ten Brink (1999), Three-dimensional velocity structure of Siletzia and other accreted terranes in the Cascadia forearc of Washington, *J. Geophys. Res.*, *104*(B8), 18,015–18,039.
Pierce, K. L., and L. A. Morgan (1992), The track of the Yellowstone hot spot: Volcanism, faulting, and uplift, in *Regional Geology of Eastern Idaho and Western Wyoming*, edited by P. K. Link, M. A. Kuntz, and L. B. Platt, *Mem. Geol. Soc. Am.*, *179*, 1–53.
Rosenfeld, C. (1985), Landforms and geology, in *Atlas of the Pacific Northwest*, edited by A. J. Kimerling and P. L. Jackson, p. 40, Oreg. State Univ. Press, Corvallis, Oreg.
Roth, J. B., M. J. Fouch, D. E. James, and R. W. Carlson (2008), Three-dimensional seismic velocity structure of the northwestern United States, *Geophys. Res. Lett.*, *35*, L15304, doi:10.1029/2008GL034669.
Siripunvaraporn, W., G. Egbert, Y. Lenbury, and M. Uyeshima (2005), Three-dimensional magnetotelluric: Data space method, *Phys. Earth Planet. Inter.*, *150*, 3–14.
Smith, J. T. (1997), Estimating galvanic-distortion magnetic fields in magnetotellurics, *Geophys. J. Int.*, *130*, 65–72.
Soyer, W., and M. Unsworth (2006), Deep electrical structure of the northern Cascadia (British Columbia, Canada) subduction zone: Implications for the distribution of fluids, *Geology*, *34*, 53–56, doi:10.1130/G21951.1.
Stanley, W. D., W. D. Mooney, and G. S. Fuis (1990), Deep crustal structure of the Cascade range and surrounding regions from seismic refraction and magnetotelluric data, *J. Geophys. Res.*, *95*(B12), 19,419–19,438.
Wannamaker, P. E., J. R. Booker, A. G. Jones, A. D. Chave, J. H. Filloux, H. S. Waff, and L. K. Law (1989), Resistivity cross section through the Juan de Fuca subduction system and its tectonic implications, *J. Geophys. Res.*, *94*(B10), 14,127–14,144.
Wannamaker, P. E., et al. (2008), Lithospheric dismemberment and magmatic processes of the Great Basin–Colorado Plateau transition, Utah, implied from magnetotellurics, *Geochem. Geophys. Geosyst.*, *9*, Q05019, doi:10.1029/2007GC001886.
Wells, R. E., C. S. Weaver, and R. J. Blakely (1998), Fore arc migration in Cascadia and its neotectonic significance, *Geology*, *26*, 759–762.

G. D. Egbert, College of Oceanic and Atmospheric Sciences, Oregon State University, 104 CAS Administration Building, Corvallis, OR 97331, USA. (egbert@coas.oregonstate.edu)
P. K. Patro, National Geophysical Research Institute, Uppal Road, Hyderabad A.P., 500 007, India. (patrobpk@ngri.res.in)